

Error quantification of particle position estimation on colour images for Particle Tracking Velocimetry

Christoph Roloff^{1,*}, Katharina Zähringer¹, Dominique Thévenin¹

1: Institute of Fluid Dynamics and Thermodynamics, Otto-von-Guericke University, Magdeburg, Germany

* corresponding author: christoph.roloff@ovgu.de

Abstract Particle Tracking Velocimetry relies on an accurate determination of particle image centroids in order to carry out reliable 3D photogrammetric reconstruction and trajectory linking. Centroid estimation on monochrome images is usually carried out with subpixel accuracy. When utilising differently coloured tracer particles to facilitate assignment procedures for PTV, colour cameras are required. They feature Bayer mosaic colour filters, which reduce the apparent pixel resolution of each colour channel.

The present work is a first approach allowing to quantify centroid errors for different combinations of centroid estimators and demosaicing procedures using simulated colour particle images and varying parameter sets. The centroid of mass estimator turns out to be the most reliable method for most demosaicing techniques, with mean errors in subpixel range. A customised colour defiltering approach seems to be superior in certain defined ranges of wavelengths, but requires a colour classification of particles a priori.

1. Introduction

Particle Tracking Velocimetry (PTV) is a three-dimensional, time resolved optical flow measurement technique usually associated with a low seeding density (Raffel et al (2007)) compared to alternative techniques like Tomo-PIV. The limitations regarding the tracer number density primarily arise due to ambiguous assignments of 1) particle images in different camera views when performing the photogrammetric particle position reconstruction (spatial correspondence) and of 2) the linking of particle positions in time to construct their trajectories (temporal correspondence).

For the latter assignment, several sophisticated tracking algorithms have been introduced which rely on the particle's history, neighbourhood or other physical constraints of the flow to predict the most likely path of the particle and to reduce occurring ambiguities. The spatial correspondence can be facilitated by an increase of camera perspectives as shown in Maas et al (1993). Nevertheless, for a higher spatial discretisation of the flow to be measured, there is still much room for alternative ways in order to reduce the existing ambiguities.

Therefore, we applied a method which divides the global tracer population into distinct subpopulations, where each subgroup of tracers can be distinguished by their colour or wavelength spectrum respectively (see Tarlet et al (2012) or Bendicks et al (2011)). In the best case, the number of ambiguities per particle can be reduced by the number of different subpopulations, as the triangulation for the 3D positioning and the tracking itself can be carried out in each particle subpopulation, which is apparently much less dense than the global population (see Figure 1). The information of the class specific spectrum of each tracer has to be decoded by an appropriate colour sensitive camera.

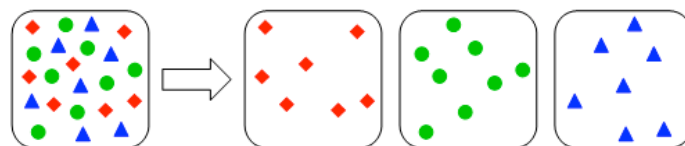


Fig. 1: Tracer subpopulations using colour classes

Nowadays, digital colour cameras usually distinguish between three colour channels, i.e. red, green,

blue, which are recorded by several methods. In a three-chip camera, the light spectrum is divided by appropriate optics (trichroic prism) and each primary colour is then recorded by a single, adequately adjusted sensor. A camera featuring the Foveon X3 Chip separates the three channels by the depth of penetration of the light sensitive substrate. The most common principle of colour cameras, however, applies a colour filter array (CFA) of red, green and blue filter elements in front of the sensor, where each pixel can only register the respective filter range. The so called Bayer mosaic is the typical spatial arrangement of those filter elements, where the amount of green pixels equals the sum of red and blue pixels to approach the human colour perception (see Figure 2). The full colour image has to be calculated as a post processing step, also referred to as demosaicing, using an appropriate interpolation method.

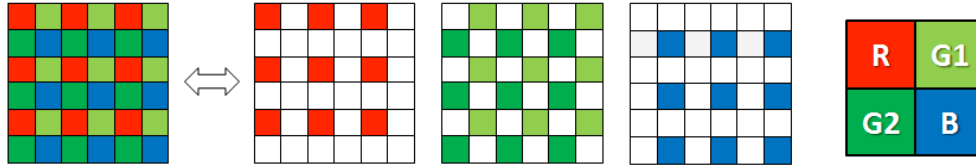


Figure 2: Bayer mosaic consisting of red, green and blue filter arrays

Due to the comparatively low costs, the Bayer mosaic can be found in the vast majority of standard digital colour cameras as well as in scientific high-speed cameras. However, an important disadvantage is the reduced spatial sampling of each colour compared to the same sized system without Bayer filter. This is especially critical when recording high frequency image scenes, like sharp edges, sudden colour changes or very tiny objects. Various algorithms that deal with advanced demosaicing techniques to compensate for the resolution issue in order to enhance image quality are available.

With respect to tracer imaging like in PTV, it is important to determine the particle position as accurately as possible. Particularly, the photogrammetric 3D reconstruction requires precise measurements of particle centres from images taken by the multi camera setup. In monochromatic imaging, centroid estimators like Gaussian fits applied to the particle image measure its centre with subpixel accuracy. However, for small particle image diameters, this is probably not applicable to colour images.

In the following, different strategies are compared to estimate quantitatively the particle centre from Bayer colour images using simulated particle images, with varying diameter, wavelength, intensity and noise levels. First, the methodology, simulation details and the applied estimation strategies are compared. Then, position measurements are presented for colour images and monochrome images, respectively. Finally, error sources and further improvements are suggested.

2. Particle simulation

Generation of artificial particle images is a widely used technique in imaging to assess measurement accuracy under controlled and predefined constraints like image diameter, intensity or noise. For our simulations, we assume a Gaussian shaped particle image with an intensity distribution:

$$I(x, y) = I_0 \cdot \exp \left[-\frac{(x - x_c)^2 + (y - y_c)^2}{2 \cdot (d_i / 4)^2} \right] \quad (1)$$

The predefined centre positions are x_c and y_c , while d_i is the definition of the particle image diameter at $I_0 e^{-2}$. The Gaussian intensity distribution is integrated over each pixel of a 9 x 9 pixel area and multiplied by a filter factor depending on the assumed wavelength of light and the pixel

colour. The simulations comprise variations of six parameters, for which details are shown in Table 1:

Table 1: parameters for particle image simulation

parameter	symbol	Range [min...step...max] or values
Centroid position	x_c, y_c	[0.00 ... 0.025 ... 0.50] px
Image diameter	d_i	[1.0 ... 0.5 ... 4.0] px
Wavelength of particle image	λ	[400 ... 25 ... 700] nm
Maximum Intensity	I_0	[250 , 500]
Filter colour of centroid pixel	pxc	[monochrome, red, green1, green2, blue]
Standard deviation of noise	σ_n	[0 , 3 , 6]

A centroid position of [0,0] refers to the exact middle point of the centroid pixel (pixel 5 in Figure 3), i.e. the pixel that covers the intensity maximum of the Gaussian bell. Centroid position variations only cover a quarter of this pixel assuming vertical and horizontal symmetry.

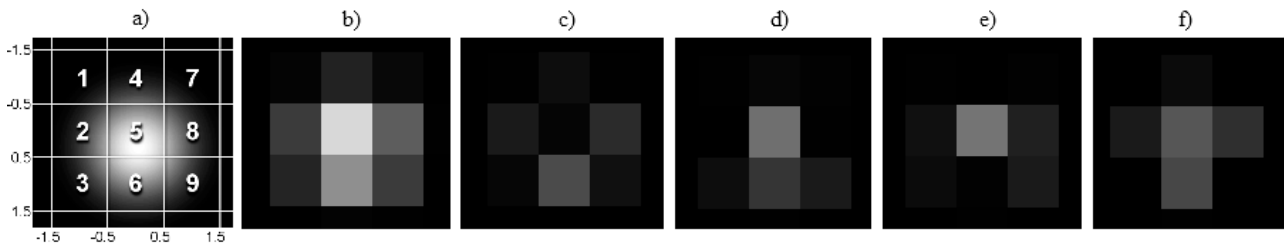


Figure 3: Simulated Gaussian bell ($d_i = 2.5\text{px}$) with maximum at [0.1 , 0.3] and corresponding pixel numeration (a); integrated and filtered images at 500 nm on monochrome pixels (b), with centroid pixel red (c), green1 (d), green2 (e) and blue (f)

The wavelength of the particle image is considered when assigning the filter factor to each pixel: Each colour filter has a specific filter value at a given wavelength (determined by the filter curve as given in Fig. 4), which is multiplied with the integrated pixel value. For example, when assuming a 525 nm particle image, monochrome pixel values are multiplied by 1, red pixels by 0.12, both types of green pixels by 0.69 and blue pixels by 0.15. Exemplary pixel intensities with different colours of the centroid pixel are shown in the middle table of Figure 4 and corresponding particle images are displayed on the right of Figure 4.

For monochrome pixels, the filter value is the same on the entire 9 x 9 pixel array. For the other colours, the centroid pixel determines the shift of the Bayer mosaic and the distribution of filter values respectively. For the sake of comparability, we define one single intensity distribution for a set of wavelength variations in such a way that the monochrome pixel at [$x_c = 0, y_c = 0, \lambda = 525 \text{ nm}, \sigma_n = 0$] has an intensity value before eight-bit digitisation of 255. Hence, colour filtering or wavelength shift produce different pixel intensity patterns as can be seen on the right of Figure 4. After filtering, Gaussian noise with zero mean intensity and varying standard deviation is added. Finally, the eight-bit discretisation limits pixel values to be in the range of [0, 255].

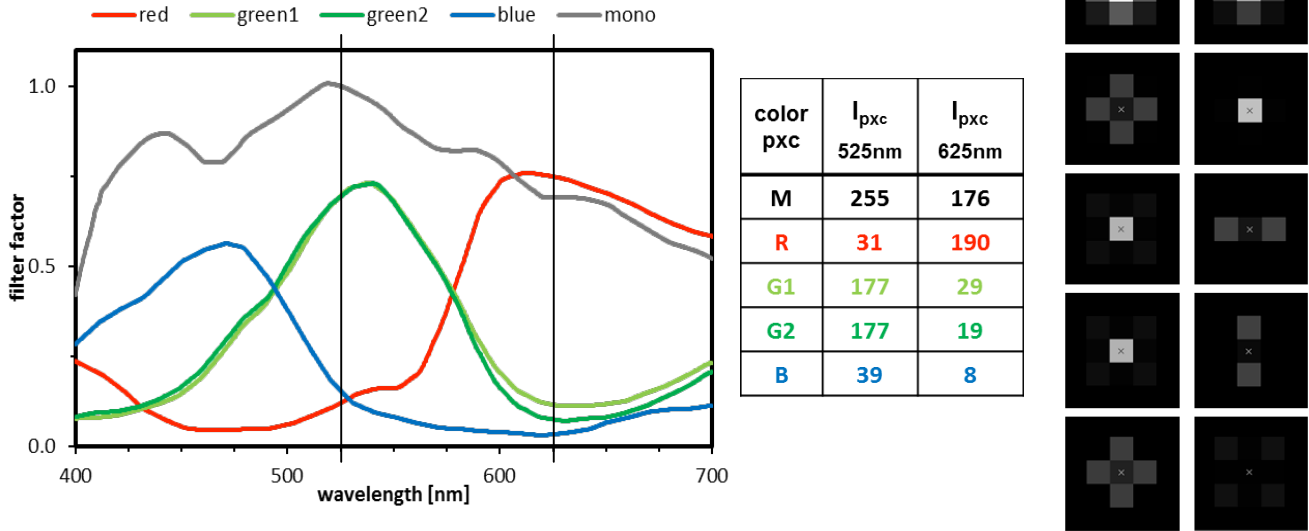


Figure 4: Left: filter curve for all five pixel colours, middle: Intensity values for centroid pixels of different colours and two different wavelengths at [0, 0] and $d_i = 2.5px$, right: corresponding pixel images

To check the accuracy of the centroid estimations, the error is defined by the Euclidean distance between the estimated position and the predefined one, whereas errors are limited to the maximum length of a pixel, i.e. $2^{0.5}$. The expected value for the error of a given parameter set is estimated by the mean of the errors of the discrete samples. The estimation of the standard deviation for this set is then given by

$$s = \sqrt{\frac{1}{N-1} \left(\sum_{i=1}^N [e_i - E]^2 \right)} \quad (2)$$

where N is the number of samples in the parameter set, e_i is the error defined by the Euclidean distance and E is the expected value of the error estimated by its mean value.

3. Centroid estimation strategies

Centroid estimation

As starting point for all estimations, the pixel values of the centroid pixel (pixel 5) and its eight adjacent pixels are considered. Thus, the calculation of particle centroids is carried out on a 3 x 3 array to keep the required data area as small as possible. Nevertheless, the basic 9 x 9 pixel array is needed for some of the demosaicing algorithms. In real camera recordings, demosaicing would be applied for the entire image and therefore it would be also influenced by nearby particles, having impact on the estimation performance. Extending the data area towards 5 x 5 pixels is possible and will certainly increase measurement accuracy, in particular for the colour images. However, it is useful to first check complex estimation strategies on a reduced particle image area, since this is more relevant for dense particle clouds and higher resolution, as found in real PTV experiments. Furthermore, in order to reduce complexity, any concerns associated to real particle images like aberrations, particle segmentation issues, peak detection or particle overlap are neglected in this first study.

Three basic centroid estimators have been applied both for colour and monochrome images:

- 1) Weighted average or “centre of mass” (COM), where the centre in x-direction x_c is written as

$$x_c = \frac{\sum_p x_p I_p}{\sum_p I_p} \quad (3)$$

The sum includes all nine pixels, with its centre coordinate x_p and its intensity value I_p . The centre of the y-direction is calculated in the same way.

- 2) Three-point Gaussian estimator (3PG), also used by Marxen et al (2000), which is the solution of the set of equations obtained when fitting a one-dimensional Gaussian to the three horizontal pixels of the 3 x 3 array. The horizontal centre estimate x_c is given by

$$x_c = \frac{\ln(I_2) - \ln(I_8)}{2(\ln(I_2) + \ln(I_8) - 2\ln(I_5))} \quad (4)$$

The vertical component is computed in analogy.

- 3) Marxen et al (2000) also introduced a least-square fit of a circular symmetric Gaussian for the entire 3 x 3 pixel area (9PGF), which is applied as a third estimator. The objective function to be minimised is then defined by

$$f^2(x_c, y_c, I_0, \sigma) = \sum_{p=1}^9 \left(I_p - I_0 \exp \left[-\frac{(x_p - x_c)^2 + (y_p - y_c)^2}{2\sigma^2} \right] \right)^2 \quad (5)$$

The minimisation routine applied for this estimator is implemented in MatLab and involves the Nelder-Mead Simplex algorithm, for which details can be found in Lagarias et al (1998).

Demosaicing

Demosaicing is still a topic of high interest in image processing, since many recent publications can be found. Xin et al (2008) provide a comprising overview over recent approaches. In the present project, three techniques are compared: 1) a single-channel interpolation method, which interpolates each colour channel separately; 2) a sequential demosaicing method, which additionally takes into account possible inter-channel correlations and 3) a customised demosaicing method, which requires a previous, reliable colour classification of particles.

The single channel method is a standard bilinear interpolation (SBI) commonly used as reference interpolation, like in Longère et al (2002). The missing two colours of each pixel are linearly interpolated utilising the information of adjacent pixels featuring the requested colour. For example, to calculate the red channel of a blue centroid pixel, the values of adjacent red pixels, i.e. pixel 1, 3, 7 and 9 are interpolated. The method needs a 5 x 5 pixel matrix to demosaic the central 3 x 3 array.

The sequential method, in the following referred to as Pei-Tam-Interpolation (PTI), is adapted from a publication of Pei et al (2003). Like most sequential methods, it tries to recover the luminance channel (green) first, because its information density is doubled compared to the red and blue (chrominance) channels. In a second step, interpolation on colour differences $d_{RG}=R-G$ and $d_{BG}=B-G$ is carried out, assuming a constant spatial distribution of colour ratios. The missing information of the R and B channels is finally extracted by adding back the G channel. Further details can be found in Pei et al (2003). For reconstruction of the 3 x 3 pixel array the underlying 9 x 9 pixel values are used.

The customised demosaicing, which we call Colour Class Correction (CCC), is more a defiltering process than an interpolation. It requires a particle image that has already been assigned to a colour or wavelength class. Since a reliable classification of particle images is a basic need for the reduction of ambiguities in the PTV application and has to be carried out anyway, there is no additional effort required for this method. However, the applicability of this technique is connected to the accuracy of the classification process. In our simulation, the wavelengths to be tested are assigned to three classes as follows:

- Blue: 400 nm, 425 nm, 450 nm, 475 nm
- Green: 500 nm, 525 nm, 550 nm
- Red: 575 nm, 600 nm, 625 nm, 650 nm, 675 nm, 700 nm

For each class, a characteristic wavelength (CW) is defined, for which the reciprocals of the pixel filter factors deliver the characteristic demosaicing factors. The demosaicing factors are then multiplied by the respective pixel values on the Bayer raw image to reconstruct the pixel distribution of the original Gaussian particle image. In our case, the characteristic wavelengths are 612 nm for red, 540 nm for green and 471 nm for blue. Clearly, the choice of the CWs and the width of the emitted light spectrum of the particles are crucial parameters for the accuracy of the method. Ideally, the CWs should be as close as possible to the expected wavelengths of the seeding particles and the width of the spectrum should be as small as possible. For fluorescent particles with defined emission characteristics this seems to be a feasible constraint.

Strategy matrix

The combination of the centroid estimation with the demosaicing defines several sets of colour centroid estimation schemes, which are summarised in Table 2. All tested combinations are marked in this table. From both demosaicing interpolations, i.e. SBI and PTI, the green channel (G SBI / G PTI) and the processed greyscale image (GS SBI / GS PTI) have been used for centroid estimation. The greyscale values for each pixel are computed out of the three colour channels of the pixel by

$$I_{BW} = \frac{1}{4}I_R \cdot \frac{1}{2}I_G \cdot \frac{1}{4}I_B. \quad (6)$$

Slightly different weights instead of $\frac{1}{4}$ and $\frac{1}{2}$ have been also tested for the colour channels. However, only negligible differences in overall performance have been obtained, so that Eq.(6) has been finally retained throughout.

Table 2: Estimation strategy matrix: abbreviations are explained in the text.

	Mono	BAY	GS SBI	GS PTI	G SBI	G PTI	CCC
COM	x	x	x	x	x	x	x
3PG	x		x	x	x	x	x
9LSF	x	x	x	x	x	x	x

4. Results

To compare different procedures in a convenient manner, a suitable data averaging must first be identified. As particles moving with the flow will be imaged on different sensor positions during acquisition, the probability, that each particle is covered by red, green and blue centroid pixels is

high. Therefore, we finally average the error over the four different colours of the centroid pixel times the 441 simulated centre positions for a quarter of a pixel. The result of this averaging process is called mean error in the following.

Exemplarily, in Figure 5, the error (averaged error of the 441 positions) for the R, G1, G2 and B centroid colour is shown using a bilinear demosaiced greyscale image and the centre of mass estimator. The additional black curve displays the mean error (averaged over 441 positions times all four colours). Error bars indicate respective standard deviations. Although the averaging of centroid colours is convenient, it can be seen, that the colour of the centroid pixel will indeed have an impact on the performance, since it does not only determine the filter factor of the pixel covering the brightest parts of the Gaussian bell, but it also determines the shift of the Bayer pattern relative to the particle image. This is particularly visible for centroid pixel colours of red or blue. In both cases, there will be no similar coloured pixel inside the 3 x 3 area, while the remaining colours are sampled at least four times. The resulting error drift for blue and green pixels in the blue and red wavelength ranges can be observed for the case of a bilinear demosaiced image and centre of mass estimator in Figure 5.

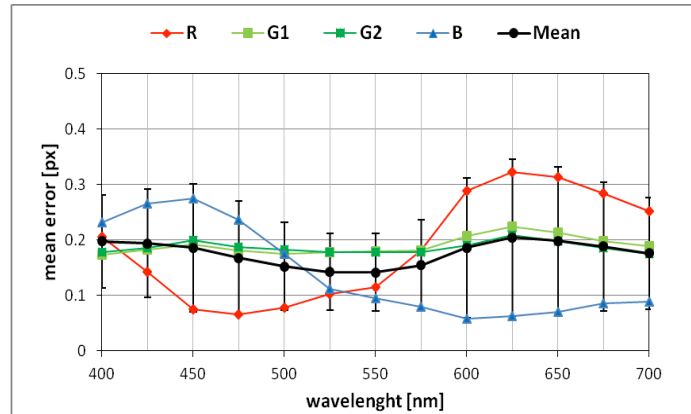


Figure 5: Mean error depending on image wavelength and centroid pixel colour for $d_i = 2.5$ px, $\sigma_n = 3$, centre of mass (COM) applied on bilinear greyscale image (GS SBI). According to the centroid colour, the R, G1, G2, B curves display the error averaged over 441 position samples. The black curve displays the mean error over 441 samples times 4 colours (R, G1, G2, B). Error bars indicate the estimate for the standard deviation.

After testing all combinations presented in Table 2, several procedures listed in the strategy matrix deliver a poor performance. In Figures 6 and 7 mean errors for all considered combinations of the strategy matrix with noise standard deviation $\sigma_n = 3$ are summarised. Figure 6 shows the results for an image intensity of 255, Figure 7 for an intensity of 500.

First, it is confirmed, that no procedure is able to reach the accuracy of estimators from monochrome images (black curves in Figs. 6 and 7). For monochromes of the 255 intensity, the 3PG and 9LSF are in particular very accurate over the entire wavelength spectrum. Contrary, for the 500 intensity images, 3PG and 9LSF feature increasing errors in the middle of the wavelength spectrum, which even increase with image diameter. This observation can be explained by pixel saturation in the wavelength range where monochrome filter factors are high (see Fig. 4) and cut down to a 255 pixel intensity. Hence, due to eight-bit discretisation, information is lost with direct impact on both Gaussian estimators.

Second, regarding the colour images, it is clearly observed that the simple and fast centre of mass method (COM) performs best for almost all demosaicing approaches. The 3PG fails to deliver reliable centre estimates in most cases. The 9LSF performs better, especially where the particle image is wide and bright on all centroid colours, i.e. in the green wavelength range, with increasing diameter and on 500 intensity images, as long as there are no pixel saturations.

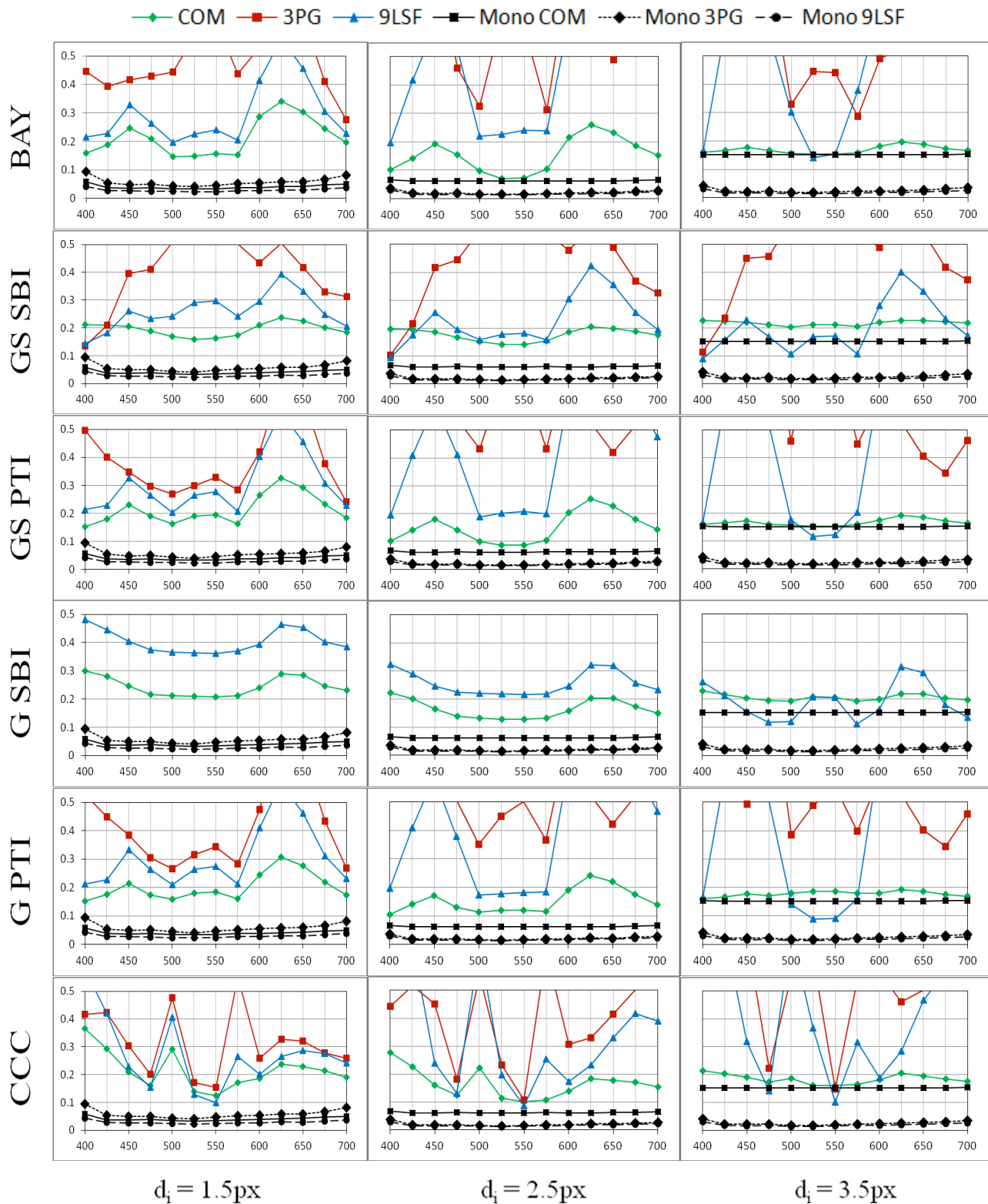


Fig. 6: Mean error of all procedures from the strategy matrix with maximum image intensity of 255 (monochrome at 525 nm before digitisation) and noise intensity $\sigma_n = 3$. Displayed on abscissas: particle image wavelength [nm]. Displayed on ordinates: mean error [px]

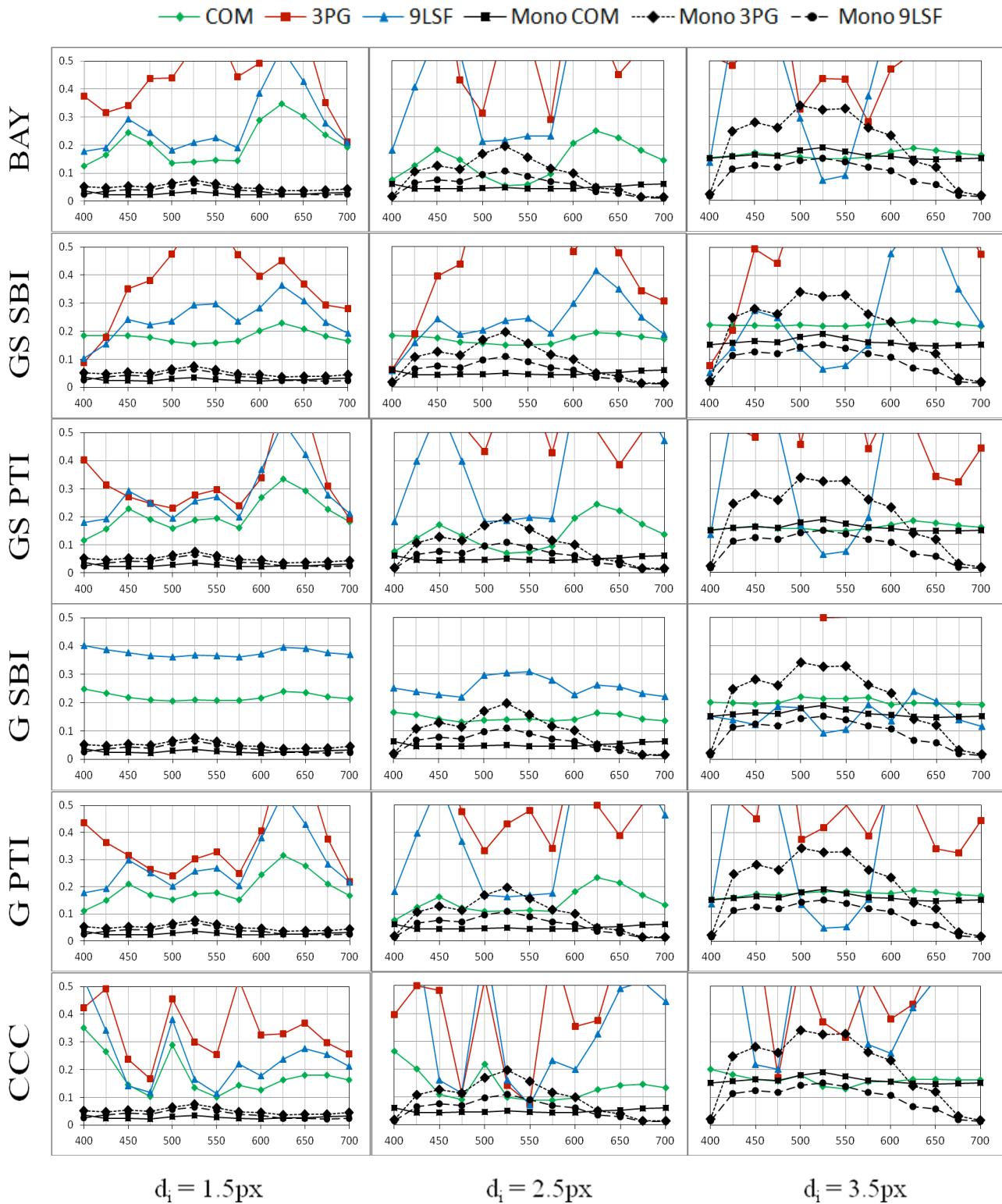


Fig. 7: Mean error of different procedures from the strategy matrix with maximum image intensity of 500 (monochrome at 525 nm before digitisation) and noise intensity $\sigma_n = 3$. Displayed on abscissas: particle image wavelength [nm]. Displayed on ordinates: mean error [px]

Using the weighted average estimator (COM), even working directly on Bayer raw images appears to be feasible over the entire wavelength range, if the image diameter is large enough to deliver strong signals for all nine pixels. The bilinear demosaicing is superior to the PTI interpolation as its performance is less influenced by the wavelength. It can also be seen that an estimation on the green channel generally delivers higher accuracy compared to a greyscale interpolation. Figure 8 (left) reveals the dependence of accuracy on image diameter for several procedures using the COM estimator. While for monochrome images the optimum diameter can be found at 1.5 to 2 pixels, the PTI approach and BAY need at least 2.5 pixels. An optimum for the SBI approach lies between 2 and 2.5 pixels. In Fig. 8 right, errors are plotted versus noise level for selected procedures. As expected, it can be found that there is a constant decrease of accuracy with noise level for colour approaches as well as for the monochrome estimator.

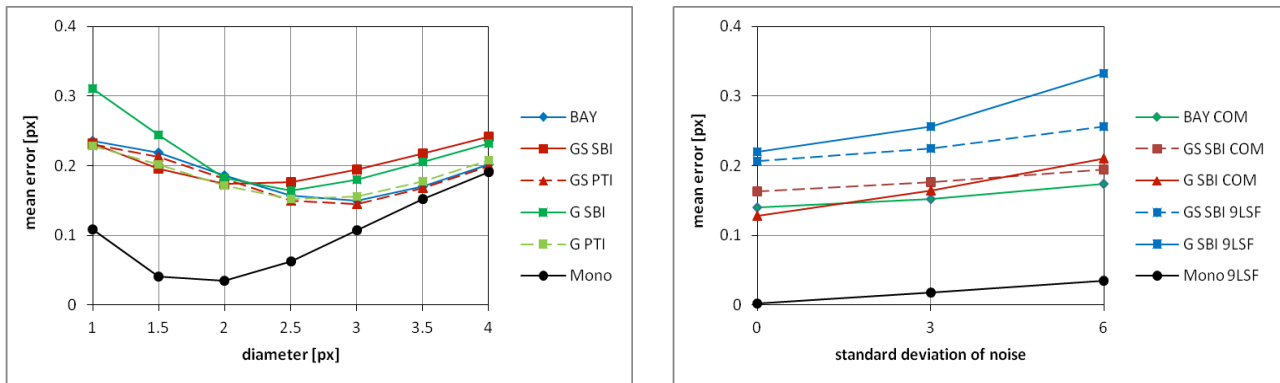


Fig. 8: Left: mean error (averaged over 441 positions times 4 centroid colours times 13 wavelength samples) vs. diameter for COM estimator on 255 intensity images with noise $\sigma_n = 3$. Right: mean error (averaged over 441 positions times 4 centroid colours times 13 wavelength samples) vs. diameter for selected procedures from strategy matrix on 255 intensity images with noise $\sigma_n = 3$.

Furthermore, Figures 6 and 7 reveal, that it is worth spending attention towards the performance of the customised demosaicing approach (CCC). It is almost completely useless at wavelengths that are not in close vicinity to the characteristic wavelength (CW) of a class. However, at wavelengths which roughly match the CWs, the mean error decreases rapidly. For example in 255 intensity images, the wavelength of 550 nm, which is close to the CW of green of 540 nm, the mean error of 0.085 px using CCC 9LSF for an image diameter of 2.5 px almost reaches the COM mean error of 0.061 px on monochrome images. At 475 nm, which is very close to the CW of blue (471 nm), we find another minimum of error using CCC 9LSF. Since the discretisation range of eight bits is not fully used in the 255 intensity images, even better results can be found in images with intensity 500. The minimum for the red class can be identified at 600 nm. However, the mean error is comparatively high, which might be caused by the strong gradient in both green filter curves at this wavelength, leading to erroneous defiltering factors compared to defiltering factors of the class-characteristic wavelength.

As mentioned previously, the choice of the characteristic wavelength is crucial for a success of this approach. If the defined spectra of different fluorescent colours would be used for colour PTV in real experiments, the CWs of each class could be fixed at high peaks of the emission spectrum. Instead of prescribing defilter factors at one single CW, it could also be useful to choose each defilter factor to be a characteristic mean of its class, covering most possible emission wavelengths and thus minimizing defiltering errors.

5. Summary

Errors for particle centroid estimators on Bayer colour images have been quantified considering

different demosaicing approaches acting on simulated particle images. The demosaicing with standard bilinear interpolation and sequential interpolation introduced by Pei and Tam (2003) is not able to sample the Gaussian image in a reliable manner, and thus leads to poor performance on most parameter sets. However, a simple centre of mass estimator (COM) shows subpixel accuracy for a wide range of different parameters and seems suitable as an estimator on a low-size sampling of 3×3 pixels. Nevertheless, the estimation accuracy does not reach the level obtained by monochrome images providing full pixel resolution. An alternative defiltering approach (CCC), which tries to reconstruct the pixel intensities before colour filtering, performs very well in certain parameter ranges of parameters using the least-square Gaussian fit or the centre of mass method. However, and in contrast to all other approaches, the CCC defiltering requires a reliable colour classification before starting the process. When the colour of the particle image has been suitably identified, CCC is able to correct the pixels for filter factors. The involved colour classification is challenging, but is needed for colour PTV anyway.

It has to be noted that finding particle images in real experiments on Bayer images requires an additional image processing step before estimation of the particle centroid. Furthermore, a segmentation procedure has to be carried out, which might deliver more or less pixels than a 3×3 array for a single particle image, depending on the segmentation algorithms. In previous works, bilinear demosaicing and greyscale transformation have been used in a first step to find particle images and corresponding peaks. Dynamic threshold segmentation on these greyscale images and a COM estimator then delivered particle centres. Finally, an Artificial Neural Network was applied for colour classification. Using the CCC 9LSF it seems possible to improve particle centre estimation and to enhance the accuracy of 3D photogrammetric triangulation procedure. However, additional tests are still required to better characterise the performance of the CCC defiltering applied to real images.

Additionally, the feasibility of extending the estimator data towards an area larger than 3×3 pixels should be evaluated, since it might improve noticeably the accuracy. Overlapping particles have to be considered in this case, which might lead to further problems. Since Artificial Neural Networks are already implemented for colour classification, they might perhaps be used as well for segmentation and centre estimation based directly on Bayer images.

References

- Bendicks, C., Tarlet, D., Roloff, C., Bordás, R., Wunderlich, B., Michaelis, B. and Thévenin, D., (2011) Improved 3-D Particle Tracking Velocimetry with coloured particles. *J. Signal Inform. Proc.* 2: 59-71
- Lagarias, J.C.; Reeds, J.A. ; Wright, M.H.; Wright, P.E. (1998) Convergence Properties of the Nelder-Mead Simplex Method in Low Dimensions. *SIAM J. Optimization*, 9: 112–147
- Li, X.; Gunturk, B.; Zhang, L. (2008) Image Demosaicing: A systematic survey. *Proc. of SPIE-IS&T Electronic Imaging*, 682211J: 1-15
- Longère, P.; Zhang, X.; Delahunt, P.B.; Brainard, D.H. (2002) Perceptual assessment of demosaicing algorithm performance. *Proc. IEEE*, 90: 123-132
- Maas, H.G.; Gruen, A.; Papantoniou, D. (1993) Particle Tracking Velocimetry in three-dimensional flows, Part 1. Photogrammetric determination of particle coordinates. *Experiments in Fluids* 15: 133-146
- Marxen, M.; Sullivan, P.E.; Loewen, M.R.; Jähne, B. (2000) Comparison of Gaussian particle

center estimators and achievable measurement density for Particle Tracking Velocimetry.
Experiments in Fluids 29: 145-153

Pei, S.-C.; Tam, I.-K. (2003) Effective color interpolation in CCD color filter arrays using signal correlation. IEEE Trans., 13: 503-513

Raffel, M.; Willert, C.E.; Wereley, S.T.; Kompenhans, J. (2007) Particle Image Velocimetry, Springer, Berlin

Tarlet, D.; Bendicks, C.; Roloff, C.; Bordás, R.; Wunderlich, B.; Michaelis, B.; Thévenin, D. (2012) Gas flow measurements by 3D Particle Tracking Velocimetry using coloured tracer particles. Flow, Turbulence and Combustion, 88: 343-365